

Critical current stability of 2G REBCO tape for space-flight HTS leads

Edgar R Canavan and Brian Comber

NASA Goddard Space Flight Center, Code 552, Greenbelt, MD 20771 USA

Email: Edgar.R.Canavan@nasa.gov

Abstract. High reliability is an essential requirement for all spaceflight hardware. Like the Hitomi x-ray observatory, its follow-on mission XRISM uses 2G REBCO tapes as current leads for the superconducting magnets that are a key component of the Adiabatic Demagnetization Refrigerator (ADR) that cools the detector array. While the Hitomi Soft X-ray Spectrometer (SXS) worked flawlessly in orbit, during its development there were indications that the critical current of its specialized REBCO tapes could degrade over time when exposed to normal-humidity air. To demonstrate that the updates to the XRISM HTS lead assemblies had mitigated this risk, a series of tests were carried out to measure the stability of I_c of dozens of samples over a period greater than the flight assemblies were exposed to air during integration and test. The test rig allowed not only the measurement of the sample I_c , but also the localization of the voltage rise as the current approached I_c . We will discuss the trends in the critical current of the samples, as well as localization of lower I_c regions.

1 Introduction

RESOLVE is a soft x-ray spectrometer capable of accurately measuring the energy of each photon hitting its detector. The detector, an array of microcalorimeters, operates at a temperature of 50 mK to achieve its extraordinary energy resolution [1]. RESOLVE is one of two instruments on the X-Ray Imaging and Spectroscopy Mission, and is a near duplicate of SXS, one of four instruments on the Hitomi satellite. Hitomi launched in February 2016, and SXS worked flawlessly in orbit for nearly a month before an attitude control system software issue caused the mission to be lost [2, 3]. Like SXS, RESOLVE uses a complex, fault tolerant cryogenic system. A three stage Adiabatic Demagnetization Refrigerator (ADR) provides the thermal environment for the detector array. It lifts heat from 50 mK and discharges it to either a superfluid helium bath at 1.2 K or a Joule-Thomson cryocooler nominally at 4.5 K. The superconducting solenoids that drive the ADR stages require currents up to 2 Amperes [4]. The necessity of low parasitic heat leak onto the helium tank and the JT-cooled stage demand the use of High Temperature Superconductor (HTS) leads between the ADR magnets and a shield cooled by two Stirling-cycle refrigerators, which nominally operate around 28 K. The SXS HTS lead assemblies used 1 mm wide 2G REBCO tape. Tapes were supported by carbon fiber composite structure. Printed Circuit Boards (PCBs) at either end accommodated the transition to the NbTi magnet leads at the cold end and a normal harness at the warm end [5]. The HTS lead assemblies are not redundant. Thus, a loss of function would mean a loss of the entire instrument.



While the RESOLVE HTS lead assemblies were mechanically identical to those of SXS, a number of issues that arose in the development of the SXS assemblies drove process changes to improve reliability and reduce risk. Early versions of the assemblies showed degradation of solder joint conductance with time. Analysis of solder joint samples showed that diffusion of indium from the indium-silver solder into Ag5%Au layer protecting the REBCO led to direct contact of indium with the REBCO layer, which is known to degrade the I_c [6]. This problem was avoided for RESOLVE by plating the regions of the tape around the solder joint with a heavy ($\sim 20\ \mu\text{m}$) layer of copper, which effectively blocked indium diffusion, while maintaining the very low thermal conductance of the unplated tape between the solder joints. In addition, a new soldering rig was developed that enabled careful control of the temperature, pressure and time to improve the repeatability of solder joint conductances.

The other issue encountered with one set of SXS lead assemblies was a major loss of I_c after ~ 1 year in storage, from > 16 Amp (77 K, LN_2) measured after slitting to < 5 Amp (65 K, vacuum). For SXS, 1 mm wide tape was produced by cutting commercially available 12 mm wide tape. This process left the edges of the tape exposed. There was a concern that lateral diffusion of H_2O and CO_2 from the edges into the REBCO layer caused degradation of I_c . Measurements on a few tapes stored in vacuum, in a dry box, and in a normal laboratory environment showed different critical current degradation behavior. Tapes stored in vacuum showed no I_c degradation, some tapes stored in lab air showed substantial degradation, while those stored in a dry box had smaller, but measurable degradation. There was wide sample-to-sample variation in the tapes stored in an uncontrolled laboratory environment; some showed only $\sim 1\%$ loss after 8 months, while others showed $> 20\%$ loss over the same period. Two samples measured over 17 months shows $> 60\%$ decline in I_c . To eliminate the risk created by the exposed edges, for RESOLVE the tapes were recoated with Ag5%Au immediately after slitting, as is standard for most commercially available tape widths less than 12 mm. However, the lateral diffusion hypothesis was not definitively proven, and there was concern that there are other degradation mechanisms, such as by diffusion through pinholes in the Ag-Au coating. The critical current of REBCO tape is often limited by small regions of lower J_c . In wide tapes, the current flows around these regions, so they have little impact. However, in 1 mm wide tapes, a region of lower J_c even just a few hundred micrometers wide can have a strong effect on I_c . Throughout the project, precautions were taken to minimize exposure to air. Tape sections were stored in vacuum after receipt from the manufacturer, and completed HTS lead assemblies were stored in vacuum until installation into the flight cryostat. However, exposure is inevitable during the lengthy (several month) assembly and close-out of the cryostat. In RESOLVE, this period was extended by many more months due to a difficult-to-locate leak. Because of the residual concerns over I_c degradation due to air exposure, an effort was made to measure changes in the I_c of tapes samples exposed to air.

2 Materials and Methods

2.1 HTS Samples

All samples used in this study were manufactured by SuperPower in January of 2018 from 12 mm wide Ag5%Au coated REBCO tape. Many meters of this tape were slit to 1 mm in a proprietary process developed for this application and were recoated with Ag5%Au. From this stock, a few dozen sections were cut to the specific lengths needed for the HTS lead assemblies and both ends were plated with a $20\ \mu\text{m}$ layer of copper so as to leave a span of 589 mm between the printed circuit boards unplated. The manufacturer tested the critical current of each section up to 20 Amp, and those with critical current greater than 16 Amp were delivered to NASA in February 2018 and were immediately put in a vacuum chamber for storage. The remaining stock of slit tapes was stored in normal room temperature air by the manufacturer. Of the tapes delivered in the first batch, only those that showed no measurable voltage rise up to the 20 Amp manufacturer test limit were used in the fabrication of the flight assemblies. Functional testing of the flight HTS lead assemblies is performed in vacuum, and the instruments limit the maximum current applied to 5 Amp, so the critical current of the flight tapes are not known. Several

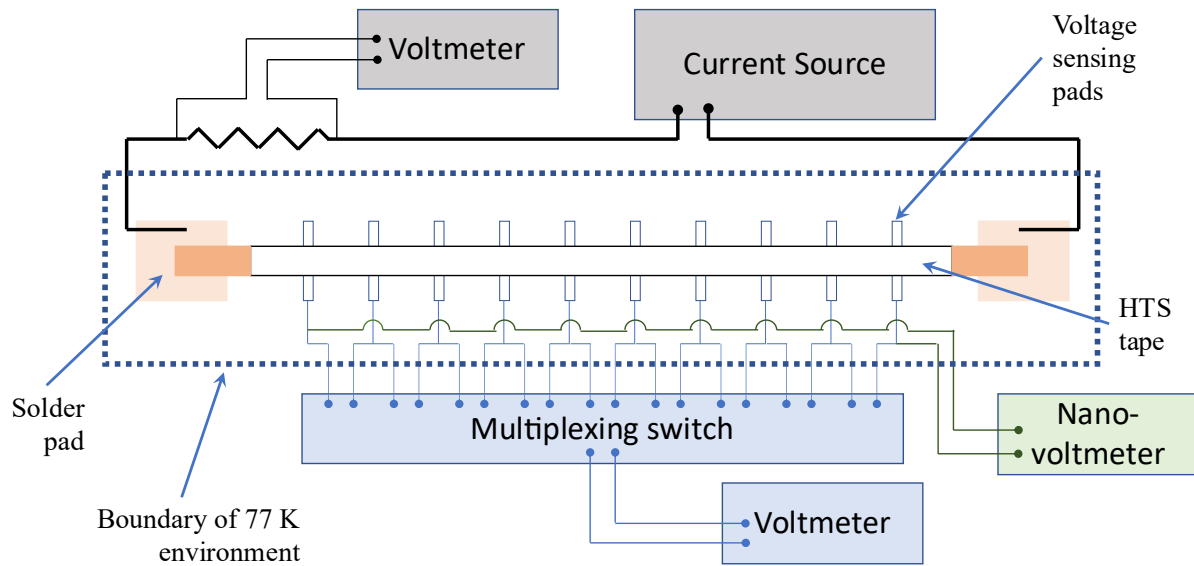


Figure 1. A schematic of the measurement apparatus. The region inside the dashed line represents one of 12 units on the printed circuit board.

tapes from this first batch, however, were used for preliminary I_c testing units after the flight build was completed.

For more extensive I_c testing, an additional batch of 48 tape sections was procured. These sections were fabricated from the 1 mm material originally produced in January 2018. They were cut to length and plated on the ends according to the same specifications as the first batch. As before, the $I - V$ measurements were made up to 20 Amp, and only sections that showed no transition below 20 Amp were counted toward the 48. It was noted that yield was very dependent on handling, with greater yield achieved as process improvements were made.

2.2 Test apparatus

Preliminary critical current tests were done on a simple rig consisting of a sheet of G-10 fiberglass with copper plates at either end to allow attachments of the current leads. Solder joints were made to these plates using the same soldering process as was used for the flight assemblies. Fine stainless steel wires were directly soldered to the tapes inboard of the high-current solder joints for sensing the voltage rise across the tapes. Measurements were made in a large flat foam tub with a foam cover, which was filled with liquid nitrogen to a level at least 1 cm above the tapes. Current was supplied by a superconducting magnet power supply (Cryomagnetics CS-4) which was capable of 50 Amps. It operates in a current source mode. The magnet power supply had a quench protection circuit which rapidly turned off the current if a rapid voltage rise was detected. Current was measured by a precision shunt and a 6.5 digit multimeter (Keithley 2000). Voltage across the taps was measured with a 7.5 digit nanovoltmeter (HP 34420A).

After the initial I_c measurements, more capable test rigs were developed. These were large printed circuit boards. Each was capable of accommodating 12 tapes. Each tape had 10 contact pads, and small clamps held the tape against the pads at these points. These contacts allowed the voltage across 9 separate sections of the tape to be measured, thus allowing the voltage rise in the tape to be localized. As with the initial test, copper sheets at each end supported connections between a heavy copper lead and the HTS tape. The solder joint to the HTS tape was made using the same procedure as was used on the flight assemblies. A schematic of the critical current test is shown in figure 1. The same instrumentation was used for the measurement as described in the previous paragraph, except that the 9 voltage tap pairs were connected through a multiplexer switch to a 6.5 digit multimeter. Wiring on the board also allowed

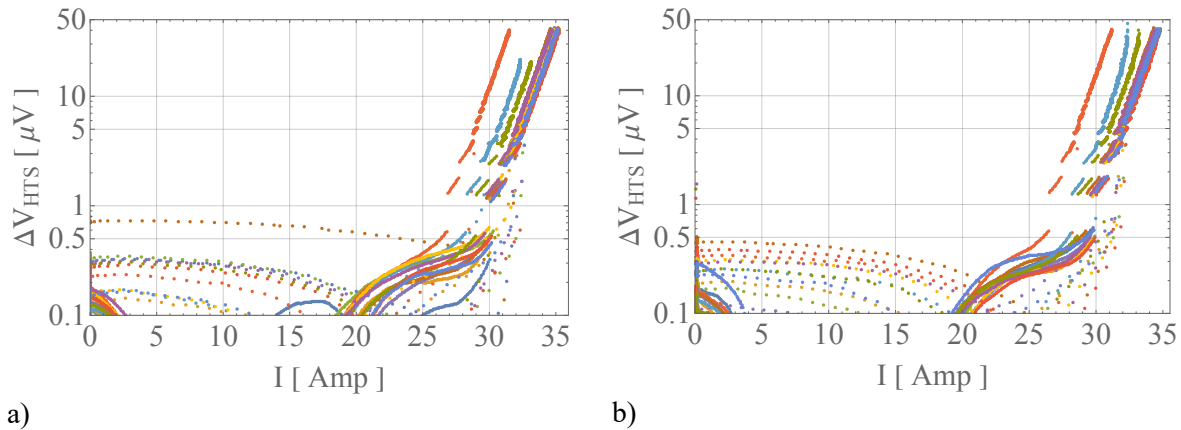


Figure 2. Voltage rise as a function of current for the 12 sample HTS tapes on board 12-2 for measurement runs on a) 2022-03-16 and b) 2022-04-22. In a), two tapes (shown in light blue and olive green) quenched before reaching the 40 μV limit. The gaps in the curves are presumably caused by sudden flux motion.

the outermost voltage taps to be continuously monitored by the 7.5 digit multimeter. Because of delays due to the COVID pandemic, only two of these boards were populated and tested.

Measurements were automated to improve repeatability, although variation between samples prevented perfect replication of the measurement process from sample to sample. The algorithm first made a 30 second average of the voltage across the outermost voltage taps with no current applied. This voltage offset, presumably due to thermal EMF, varied between samples by $\pm 30 \mu\text{V}$, but was repeatable from run to run over the course of months. Then, using the multiplexer, the baseline voltage across the 9 individual tape sections was measured. Current was then ramped up at 100 mA/s until the voltage at the nanovoltmeter reached 3 μV above the measured baseline, after which the ramp rate was slowed to 10 mA/s. Ramping continued until the voltage rise above the baseline (ΔV) reached a preset maximum, or until a quench was detected. In the preliminary board, all tapes reached $> 59 \mu\text{V}$, which corresponds to the standard 1 $\mu\text{V}/\text{cm}$ definition for I_c . However, in the newer test rig, all tapes quenched at a lower voltage rise, even though in general almost all had higher I_c . For this reason, a lower voltage rise limit of 40 μV was chosen. In many cases, tapes left at this point were not stable, and would quench if left there for the tens of seconds needed to complete the measurement of the voltage across the 9 individual sections. Thus, after reaching the 40 μV voltage rise limit, the current was reduced slightly until $\Delta V = 20 \mu\text{V}$, before measuring the section voltages with the multiplexer. In some instances, a tape would quench before reaching the 40 μV limit. In these cases, the $I - V$ curve was repeated with a 20 μV limit. One tape (Tape 4B on Board 1) would quench without any significant voltage rise, indicating that the region of lowest I_c was outboard of the outermost voltage contacts. Once the voltage across the sections were measured, the current was ramped down to zero and the baseline voltage across the 9 sections was again measured.

3 Results

3.1 Critical currents

Figure 2 shows ΔV , the voltage across the outermost set of taps minus the baseline voltage, as a function of current for the 12 tapes on the second test board (designated as Board 2) for two sequential test runs on 2022-03-16 and 2022-04-22. In the later run, all tapes reached the 40 μV limit without quench, even though in the earlier run two tapes quenched before reaching 40 μV , and were retested to a 20 μV voltage rise limit. The logarithmic scale emphasizes, at least at low voltages, the sudden voltage jumps as the current changes. This is clearly quite consistent across all tapes for the first few jumps. We discuss the voltage behavior in more detail below.

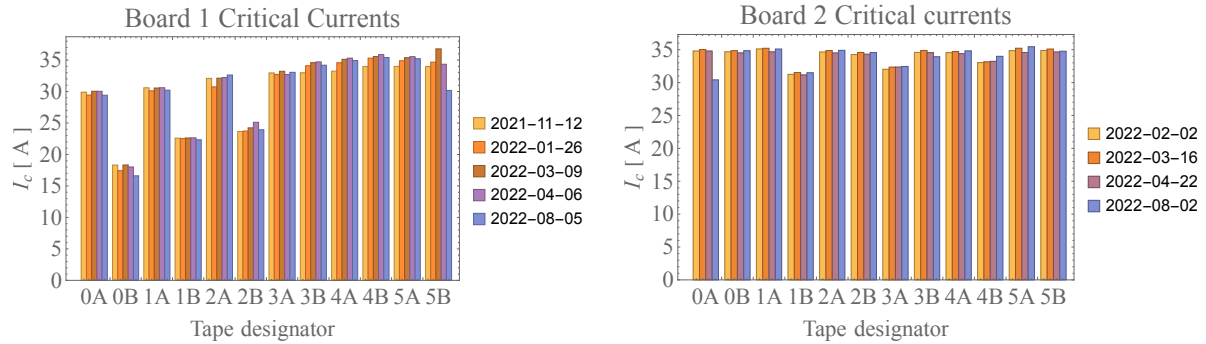


Figure 3. Critical currents for all 24 tapes and for all measurements.

We use as a measure of critical current the largest current for which $\Delta V < 40 \mu\text{V}$. With this measure, the critical currents for all the measurements of the tapes on the two boards are shown in figure 3. As can be seen, there are significant run-to-run fluctuations, both up and down, in the measured I_c , especially for board 1. The instruments used to determine the voltage and current are accurate to a small fraction of 1%, so the fluctuation cannot be explained by instrument error. As mentioned above, a number of the samples had significant run-to-run variation in the maximum voltage achieved. However, all but one consistently reached $\Delta V > 20 \mu\text{V}$. Therefore, we tested an alternate criteria for I_c : the $I - \Delta V$ with $\Delta V > 10 \mu\text{V}$ was fit to a lower order polynomial to provide smoothing. The polynomial was then solved to find the current at which $\Delta V = 20 \mu\text{V}$. Surprisingly, using this definition did not drastically reduce the variation. For most samples, the variation, as measured by the standard deviation, only decreased marginally.

Figure 4 shows the critical currents as a function of tape age, where age is computed from January 2018, when the tapes were slit and coated. The plot also includes the critical current of the 4 tapes mounted on the preliminary rig. Careful examination of the plot shows that for many of the samples, the positive and negative fluctuations in I_c are correlated, implying an uncontrolled systematic effect. However, at higher level, the figure shows that there is not a general downward trend in I_c that would

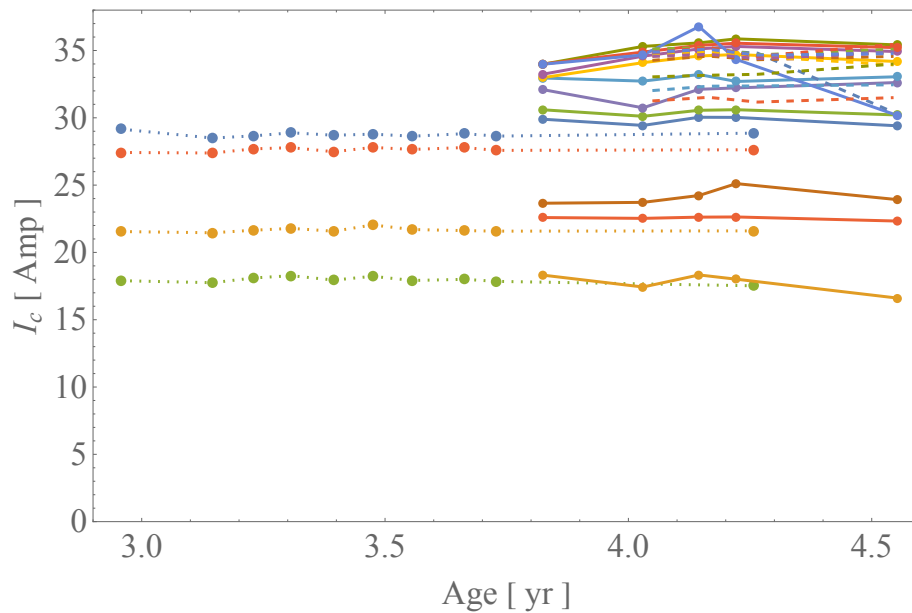


Figure 4. Critical current of all samples as a function of time since the approximate date of manufacture of the 1 mm wide tape. Solid lines: Test Board 1. Dashed lines: Test Board 2. Dotted lines: Preliminary sample test.

imply a degradation mechanism related to environmental exposure. Note that the tapes in the preliminary sample test (shown with dotted lines), which were taken from the first shipment, were stored under vacuum for most of the period from manufacture until the beginning of the test. The remaining tapes were stored in a normal indoor environment, without special humidity control, for the entire period. With a couple of exceptions, the critical currents are very steady over the period tested. There is greater evidence that changes are due to handling procedures. The seven samples with $I_c < 29$ Amp include the 4 on the preliminary board, which underwent additional manipulation as the board was reconfigured during development. The remaining three are all among the first tapes to be installed on Board 1, when the installation process was being developed. This correlates well with the observation of the manufacturer that yield improved with improved handling procedures. Note that only two of these seven have critical current that shows a definite degradation below the limit measured before shipment ($I_c < 20$ Amp). Note also that all the tapes on the second board produced have $I_c > 30$ Amp. (Although there is a nonnegligible, but small chance, $\sim 1.8\%$, that 12 samples chosen randomly from this ensemble would meet this criterion.)

3.2 Section voltage

The test boards were designed to allow localization of the voltage rise in the HTS tape samples. After the critical current determination, the current was reduced slightly so that the voltage across the outermost pads was approximately $20 \mu\text{V}$, and the voltage across each section was read out. These voltages were subtracted from measurements of the baseline or offset voltage across each section with the current at 0 Amp. Figure 5 shows the resulting voltages for fourth test of Board 2. In a tape with some damage, it is expected that the critical current is determined by a single localized region of low J_c . If this is the case, the voltage across one of these sections should be much larger than the sum of the others. Figure 6 illustrates this for all 24 samples. The charts show the maximum section voltage as a percentage of the sum of all section voltages for each tape. As expected, the three samples for which this fraction is $> 95\%$ correspond to the three tapes with critical currents well below 30 Amp. In Board 2, in which all

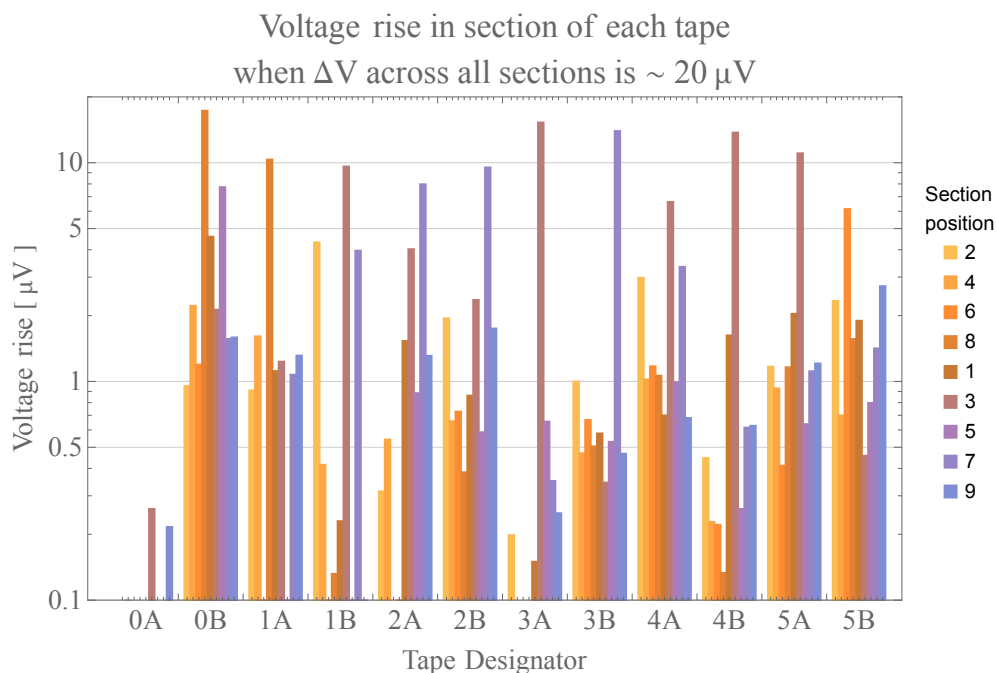


Figure 5. Voltage rise across sections of each tape with voltage across the entire tape held at $\sim 20 \mu\text{V}$. In general, the voltage across one section dominates, although in many of the samples, there is a significant voltage across multiple sections of the tape.

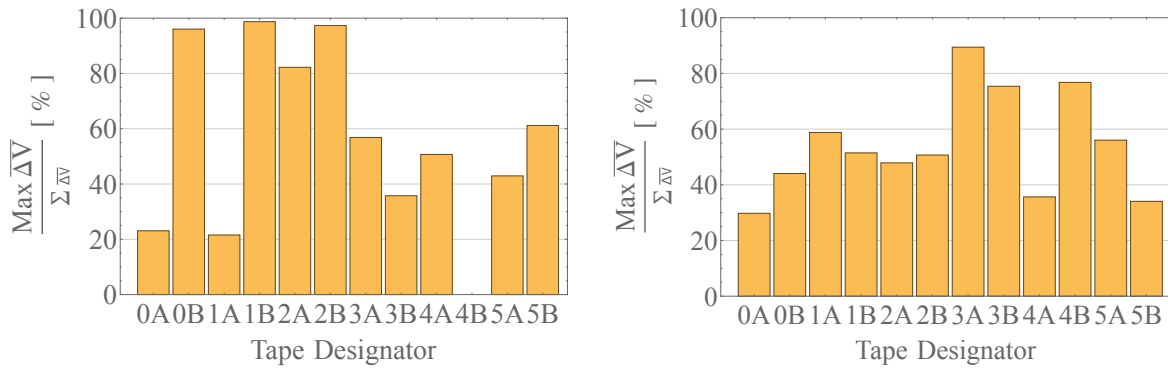


Figure 6. Maximum section voltage as a fraction of the sum of all section voltages for each tape for a) Board 1 and b) Board 2. In a), the 3 tapes in which one section accounts for more than 95% of the sum of the voltages have the three lowest critical currents.

critical currents are above 30 Amp, the maximum section voltage is a smaller fraction of the total in all cases, and there are significant voltage rises ($> 0.5 \mu\text{V}$) in multiple sections. This is an indication the current is approaching an intrinsic limit. Data for section 4B is missing because it consistently quenched before showing any voltage rise.

3.3 Voltage steps

As noted in figure 2, as the current is ramped up at a constant rate, ΔV undergoes a smooth rise, interrupted by occasional large step changes. The step changes are more easily visualized by examining the point to point change, $d(\Delta V)_i = \Delta V_i - \Delta V_{i-1}$. These step changes become very frequent as current approaches I_c , so it is convenient to plot $d(\Delta V)$ as a function of ΔV . Figure 7 shows $d(\Delta V)$ vs. ΔV plots for two sample tapes. Traces from different experimental runs are offset by $2 \mu\text{V}$ for visibility. For both samples, and over all runs, the traces start similarly, with nearly periodic steps of nearly the same magnitude. For example, for all traces shown in figure 7a), the mean peak height over the range up to $\Delta V = 20 \mu\text{V}$, is $0.75 \pm 0.05 \mu\text{V}$. Figure 7a) illustrates an example of a sample that had very regular voltage steps all the way to maximum current. Figure 7b) is the most extreme example of a tape for which the voltage steps became erratic, with large positive and negative voltage swings as the voltage rose above $\sim 18 \mu\text{V}$. This also happened to be the sample with the lowest I_c . Most samples were more similar to the one shown in figure 7a), although many did display positive and negative voltage steps of larger amplitude as they approached maximum current.

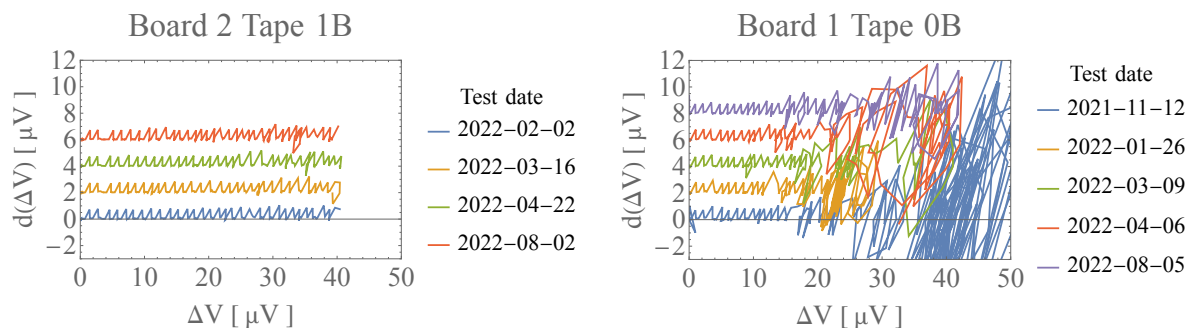


Figure 7. Point-to-point changes in the voltage rise across sample tapes, as a function of the voltage rise, for different runs. a) An example of a sample for which voltage steps are very regular and of approximate constant size. b) An extreme example of how the regularity breaks down in certain samples at higher ΔV , with large positive and negative voltage swings.

4 Conclusions

From the data obtained in these measurements, we can conclude that the probability that critical current degradation will affect the performance of the HTS lead assemblies in RESOLVE is very low. Much of this improvement comes from manufacturing process changes since SXS. Given the long period of air exposure from the time of manufacture to the time of test, all evidence implies any degradation in the original critical current is most likely due to stresses in handling of these narrow, 1 mm wide tapes and sudden liquid nitrogen cool down, rather than to a slow process (see [6]). Indeed, the only two tape samples that showed I_c below the limit to which all the samples were tested before shipment (20 Amp) were two that were used in the development of the installation process for the test rigs; most samples had I_c well above this limit. All tapes in these tests experienced some level of stress as they were moved into and out of the Dewar, and especially as they were cooled down. The RESOLVE HTS lead assemblies are designed to minimize stresses, and they experienced minimal handling between the final pre-shipment functional tests until installation into the flight Dewar. Finally, there is a very large margin on the critical current. All I_c values measured in these tests are at 77 K, but at the highest possible operational temperature for the HTS lead assemblies, 45 K, the values are at least a factor of 4 larger [7]. Thus, even the lowest I_c values in this sample set would be far above the maximum operational current in the RESOLVE instrument, 2.1 Amp.

5 References

- [1] Ishisaki Y et al. 2018 The Resolve instrument on X-ray Astronomy Recovery Mission (XARM) *J. Low Temp. Phys.* **193** 991-5
- [2] The Hitomi Collaboration 2016 The quiescent intracluster medium in the core of the Perseus cluster *Nature* 117-121
- [3] Shirron P J et al. 2018 Design and on-orbit operation of the soft x-ray spectrometer adiabatic demagnetization refrigerator on the Hitomi observatory *J Astron. Tel. Instr. Sys.* **4** 021403
- [4] Shirron P J, Kimball M O, Wegel D C, Canavan E R, and DiPirro M J 2010, Design of a 3-Stage ADR for the Soft X-Ray Spectrometer Instrument on the Astro-H Mission *Space telescopes and Instrumentation 2010 – Ultraviolet to Gamma Ray* **7732** 773212
- [5] Canavan E R, James B L, Hait T P, Oliver A and Sullivan D F 2014 The Astro-H high temperature superconductor lead assemblies *Cryogenics* **64** 194-200
- [6] Canavan E R, Leidecker H, Panashchenko L 2015 Conductance degradation in HTS coated conductor solder joints *Advances in Cryogenic Engineering – Materials* **102** 012032
- [7] Zhang Y F, Lehner T F, Fukushima T, Takamoto H and Hazelton D W 2014 Progress in production of second generation (2G) HTS wire for practical applications *IEEE Trans. Appl. Supercon.* **24** 7500405